Temperature Prediction of Cladding in CANDU Spent Fuel Dry Storage Canister using CFD code and Uncertainty Analysis

Tae Gang Lee [a], Jae Jun Jeong [a*], Tae Hyung Na[b].
[a]*School of Mechanical Engineering, Pusan National University (PNU)*
[b]*Central Research Institute, Korea Hydro & Nuclear Power Co., Ltd*
[*]*Corresponding author: jjjeong@pusan.ac.kr*

Keywords : spent fuel, dry storage, CFD code, uncertainty analysis

1. Introduction

In Korea, CANDU spent fuel is stored dry in canisters or MACSTOR after six years of wet storage. These canisters, operational since 1987 in the Wolsung site, have a licensing period of 50 years, after which the stored fuel is planned to be transferred to a final disposal site. The primary function of the canister is to maintain the integrity of the fuel during this period [1,2].

The canister is a concrete cylindrical structure with a height of 6.5 m and a diameter of 3 m, as depicted in Fig. 1 below. The interior is lined with carbon steel. Each basket holds 60 bundles of CANDU-37 nuclear fuel, and there are nine baskets, 540 bundles, in a canister. The decay heat from the nuclear fuel is dissipated to the exterior environment through conduction, natural convection, and radiation, with all heat transfer processes being passive [1,2].

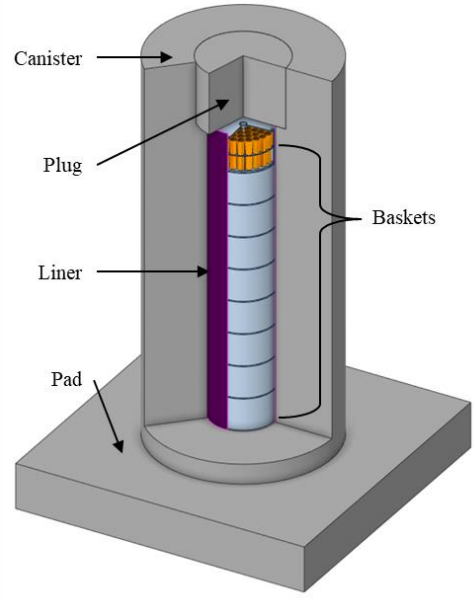

Fig. 1. Schematic of CANDU spent fuel dry storage canister.

To assess the integrity of the nuclear fuel during the licensing period, it is essential to predict the temperatures of the canister components [2]. Temperature can induce oxidation, changes in material properties, and other causing detrimental to safety. In particular, predicting the temperature of the zircaloy fuel cladding is critical. High temperatures in the cladding - and hence in the nuclear fuel - can accelerate fuel oxidation, leading to volume expansion and potentially causing radioactive material to contaminate the interior of the basket due to cladding cracking. The Safety Analysis Report (SAR) [2] limits the peak cladding temperature (PCT) to 180°C considering these physical phenomena. If the cladding temperature is low, brittleness can increase, leading to damage from minor impacts, which could be a significant safety issue during transport to the final disposal site after the licensing period. The threshold for brittleness varies with oxidation, but generally, cladding is considered brittle below approximately 55°C[3]. Therefore, predicting the temperature of the cladding is essential for safety enhancement, and both PCT and the minimum cladding temperature (MCT) must be predicted.

In this study, we used CFD code for optimal analysis and uncertainty analysis to predict the cladding temperature. Previous analyses focused only on predicting the PCT and thus were conservative [1,4]. However, as the end of the licensing period approaches, MCT has become a significant safety assessment factor, necessitating realistic optimal analysis. We have developed a CFD model for realistically thermal analyzing this canister in previous study [5,6] and utilized it in this study. To validate the results of the optimal analysis, an uncertainty assessment is essential. We classified uncertainty factors into numerical, design tolerance, code, and input uncertainties and analyzed each according to its nature. Finally, we predicted the PCT and MCT during the licensing period, considering these uncertainties.

2. Methods

In this chapter, we describe the method used in this study for predicting the cladding temperature. A flowchart is depicted in Fig. 2.

Initially, we specified the scenario. The objective of this study is to predict the PCT and MCT that could occur during the licensing period. As this period extends over 50 years, predicting cladding temperature

through transient calculations is inefficient. Therefore, steady-state calculations were performed using boundary conditions at certain time points when PCT or MCT is expected to occur. The decay heat decreases exponentially over time, being highest at the beginning of storage and lowest at the end. Considering that the heat transfer in the canister occurs passively, the ambient temperature is also a significant boundary condition. In summary, PCT is expected to occur during the summer at the beginning of storage, while MCT is anticipated in the winter at the end of storage.

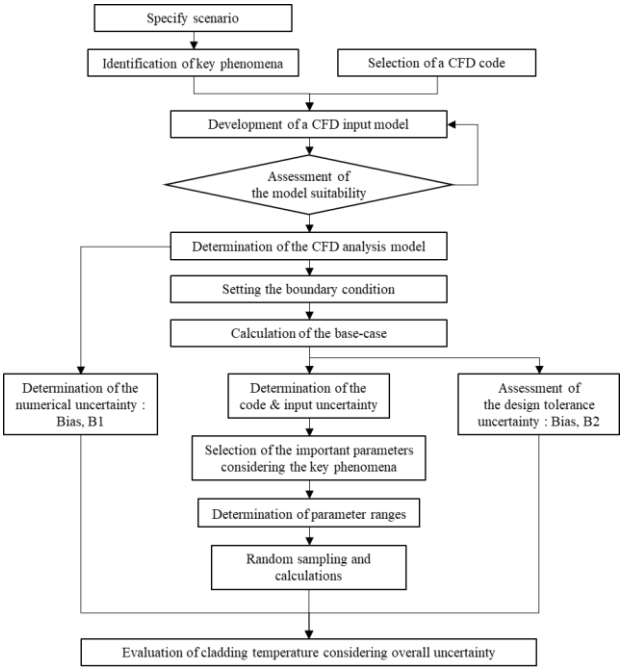

Fig. 2. Flowchart of the cladding temperature prediction.

The decay heat from the nuclear fuel stored in the canister is dissipated to the exterior environment through a combined heat transfer mechanism of conduction, natural convection, and radiation. To simulate this complex heat transfer, we derived an optimal thermal analysis model [5] using the commercial CFD code, ANSYS FLUENT 2021R2 [7]. Next, boundary conditions for the two points were derived based on the previously specified scenario, then applied to the CFD thermal analysis model to develop base-case inputs and perform calculations.

Subsequently, we conducted an uncertainty analysis. The analysis method was derived by referring to various Best-Estimate Plus Uncertainty (BEPU) methods based on KINS-REM [8–14]. We analyzed numerical uncertainty induced by the discretization process, design tolerance uncertainty based on actual canister geometry differences, code uncertainty arising from the physical models used in the analysis, and input uncertainty based on thermal properties and boundary conditions and etc. Numerical and design tolerance uncertainties were treated as biases and summed up in the final step. Code and input uncertainties were analyzed using a sampling technique applying the 3rd order Wilks formula[15]. Additionally, a sensitivity analysis was performed using Pearson's coefficient[16].

Finally, we predicted the PCT and MCT considering all uncertainties.

3. CFD Analysis

3.1 CFD Analysis Model

In the canister, decay heat is transferred to the external environment through two main steps. In the first step, heat generated from the fuel rod is transferred to the sealed basket shell through complex heat transfer processes. In the second step, this heat is then transferred from the basket shell to the outer wall of the canister and is dissipated into the external environment through convection and radiation[4,6].

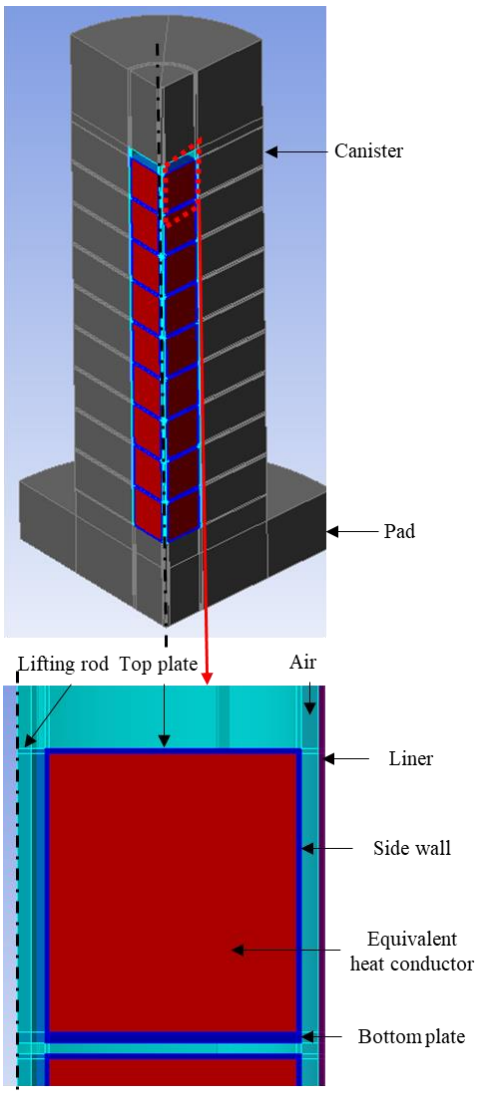

Fig. 3. The CFD thermal analysis model for the canister.

Considering all the fuel rods stored in baskets for CFD calculation would be highly inefficient and costly.

Therefore, in analysis model, the interior of the basket has been replaced with a homogeneous equivalent heat conductor (EHC) [5,6,17]. The thermal properties of this EHC were set considering the heat transfer characteristics of the actual basket. In the real basket, heat transfer occurs differently depending on the direction. Taking this into account, anisotropic thermal conductivities were applied to the EHC. The azimuth thermal conductivity was disregarded due to the axisymmetric shape of EHC. The axial effective thermal conductivity (ETC) was calculated using a weighted average based on the composition ratio of components. The radial ETC was derived by utilizing the relationship between the boundary conditions (outer wall temperature, decay heat) and the cladding temperatures derived from numerous detailed CFD analysis of the actual basket.

Fig. 3 illustrates the developed thermal analysis model for the canister [5]. For reasons of computational efficiency, a 1/4 axisymmetric assumption was applied. The geometry of the model was considered as close to the actual design as possible. Following a study on mesh independence, a mesh consisting of 4.55 million computational cells was employed. The Discrete Ordinates (DO) method was utilized for the radiation heat transfer. For modeling fluid flow within the canister, we applied the Boussinesq approximation, used an ideal gas model, and adopted a laminar flow approach as following SAR [1,2] and NUREG-2152 [18]. The computational time was approximately 3.2 hours, utilizing 12 cores of the AMD Ryzen Threadripper 3.79 GHz processor. Although this resulted in computing times that were approximately 150% of those in prior conservative studies [5], it led to significantly more precise predictions regarding the temperatures of the cladding.

3.2 Base-case Input and Calculation Results

The CFD analysis model and the boundary conditions derived through scenario were used to generate base-case inputs. The decay heat was calculated using the ORIGEN program[19], considering a burnup of 7,800 MWd/MTU[20] for the standard nuclear fuel for storage, resulting in values at the storage beginning of 364.8 W per basket and values at the end of 118.8 W per basket. Ambient temperature was determined from the last decade's meteorological data for the Wolsong site[21], with summer and winter temperatures averaging 25.7 °C and 1.24 °C, respectively. The external wall conditions of the canister were natural convection cooling and external radiation cooling established by referencing the SAR [1,4]. Solar insolation conditions were applied only to the base case input for PCT prediction, referencing 10CFR71.71.[22] Using these developed base-case inputs, calculations were performed.

In the beginning of storage, calculations revealed the PCT to be 148.0 °C, and the MCT to be 98.8 °C. As depicted in Fig. 4 (a), the highest temperature was observed in the seventh basket from the bottom, whereas the lowest was outside the bottom basket. This indicates a substantial safety margin for PCT, notably lower than 180 °C set for design criteria.

Toward the end of the storage term, the PCT was recorded at 38.8 °C, with the MCT dropping to 18.1 °C, as shown in Fig. 4 (b). Here, the highest temperature shifted to the sixth basket from the bottom, a change attributed to the significant reduction in decay heat and the consequent decrease in natural convection effects. Noteworthy is that, by the end of the storage period, both the PCT and MCT are anticipated to remain below the threshold of 55 °C, associated with brittleness.

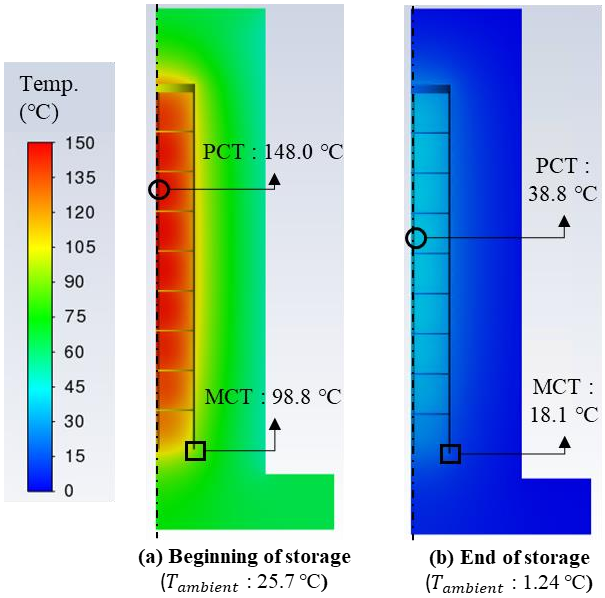

Fig. 4. The CFD thermal analysis model for the canister.

4. Uncertainty Analysis

4.1 Numerical and Design Tolerance Uncertainty

In the previous study [5], the canister CFD analysis model's mesh consisted of 4.55 million elements. The mesh independence study indicated negligible temperature variations due to mesh size, with changes in both PCT and MCT less than 0.1°C. For a conservative estimate, numerical uncertainty, labeled as bias B1 in Fig. 2, was established at +0.5°C for PCT and -0.5°C for MCT.

Per the SAR specifications [1], concrete canisters and stainless-steel baskets allow for size tolerances of 0.5% and 0.15%, respectively. Subsequent CFD simulations accounting for these design tolerances showed minimal influence on cladding temperatures, altering by no more than ±0.1°C. Conservatively, we assigned a bias B2 in Fig. 2 of +0.5°C for PCT and -0.5°C for MCT, reflecting these findings.

Table I: The uncertainty of the parameters.

No	Associated phenomenon	Parameter	PDF	Mean	Range (± 2σ)	Ref.
Code uncertainty parameters						
1	Convective heat transfer in the canister	C_1	Normal	1	[0.605, 1.395]	[8]
2	Radiant heat transfer in the canister : DO model	C_2	Normal	1	[0.95, 1.05]	[23]
Input uncertainty parameters: boundary conditions						
3	Convective heat transfer at the outer wall	C_3	Normal	1	[0.605, 1.395]	[8]
4	Radiant heat transfer at the outer wall	C_4	Uniform	1	[0.6, 1]	-
5	Decay heat per basket at the beginning [W]		Normal	364.8	[353.8, 375.8]	[19]
	Decay heat per basket at the end [W]		Normal	118.8	[115.2, 122.4]	[19]
6	Ambient temperature at summer [ºC]		Normal	25.7	[23.0, 28.4]	[21]
	Ambient temperature at winter [ºC]		Normal	1.24	[-1.98, 4.46]	[21]
Input uncertainty parameters: thermal properties						
7	Conduction	$k_{stainless\text{-}steel}$	Normal	1	[0.98, 1.02]	[24]
8		$k_{carbon\text{-}steel}$	Normal	1	[0.95, 1.05]	[25]
9		$k_{concrete}$	Normal	1	[0.95, 1.05]	[1,26]
10		k_{air}	Normal	1	[0.98, 1.02]	[27]
11		Radial ETC	Uniform	1	[0.93, 1.07]	-
12		Axial ETC	Uniform	1	[0.92, 1.08]	-
13	Convection	μ_{air}	Normal	1	[0.98, 1.02]	[27]
14	Radiation	ϵ_{basket}	Normal	0.36	[0.288, 0.432]	[1,4]
15		ϵ_{liner}	Normal	0.5	[0.4, 0.6]	[1,4]
16		$\epsilon_{canister}$	Uniform	0.9	[0.85, 0.95]	[1,4]

4.2 Code and Input Uncertainty

In this analysis, conduction, convection, and radiation are all considered critical. Therefore, the code and input uncertainty parameters were selected to account for all these modes of heat transfer. Two parameters for code uncertainty and fourteen for input uncertainty, totaling sixteen parameters, were chosen. The uncertainties of these parameters and references are summarized in Table I.

The uncertainties of most parameters were determined through literature survey, while some were decided using a conservative approach or through CFD calculations. The uncertainties of the convective heat transfer coefficients, C_1 and C_3, were applied based on the uncertainty ranges provided by KINS-REM[8]. Typically, the uncertainties of these parameters are assessed through integrated effect tests. However, as experiments on this canister are challenging, the most conservative approach was adopted. The uncertainty of the external radiation heat transfer, C_4, due to scattering or absorption in the external air was conservatively set to the range [0.6, 1.0] and assumed a uniform distribution. The uncertainty range for the ETC applied to the EHC was determined through CFD calculations. Considering the uncertainty of the detailed basket analysis, the inputs with the best and worst heat transfer scenarios were created. A number of calculations using the inputs were performed to assess the uncertainty range, and a conservative uniform distribution chosen.

We generated random samples for the listed code and input uncertainty parameters in Table 1, determining the sample size based on the third-order Wilks' formula, which required 124 samples per target. Therefore, we conducted 248 sample calculations in total, dividing them equally between estimating the PCT at storage

start and the MCT at storage end. The third highest or lowest values from the sample calculations indicate the respective PCT and MCT satisfying 95/95 criterion. The random sampling was executed using MATLAB. A sensitivity analysis was performed to assess the impact of parameters by using Pearson's coefficient.

4.3 Results

Fig. 5 shows the PCT distributions from sampling calculation results. Following the third-order Wilks' formula, the PCT satisfying the 95/95 criterion was assessed as 158.8 °C, exceeding the base case by 10.8 °C due to uncertainties, notably in radiation heat transfer at the outer wall.

The sensitivity analysis, presented in Table II, shows the significant impact of radiant heat transfer (C_4) on the PCT. Other crucial parameters include the convective heat transfer (C_3), decay heat, ambient temperature, emissivity of the canister, and thermal conductivity of concrete. The key parameters, except decay heat, primarily influence the cooling mechanism at the outer wall. This sensitivity stems from the effect of solar insolation, with the solar energy impacting the outer wall (approximately 15,062 W) vastly surpassing the internal decay heat of the canister (approximately 3,283 W). Consequently, the effectiveness of dissipating solar heat from the outer wall is pivotal in determining the PCT.

Incorporating biases B1 and B2 of +0.5 °C each, the initial storage PCT is predicted to 159.8 °C, below the 180 °C design criteria, suggesting that the fuel integrity remains secure within operational limits.

Fig. 6 presents the MCT distribution derived from the sampling calculation results. The MCT that satisfies the 95/95 criterion was identified as 15.4 °C, which is 2.7 °C lower than the base-case. Sensitivity analysis, summarized in Table III, identified ambient temperature as the most critical factor affecting MCT, with other significant parameters being convective heat transfer at the outer wall (C_4), inside the canister (C_1), and the thermal conductivity of carbon steel.

As decay heat reduces to about one-third from the start to the end of storage, internal heat transfer within the canister becomes constrained. This limitation causes the MCT to be heavily influenced by external temperatures. Previous research [5] has indicated that convective heat transfer significantly affects axial temperature distribution within the canister. At thin and elongated carbon steel liners of 1 cm thickness, heat predominantly moves in the axial direction. Given the Pearson coefficient value of these parameters, it is evident that axial heat transfer considerably determines the MCT.

Adding the biases B1 and B2, both set at -0.5 °C, to the sampling calculation results, the MCT is assessed at 14.4 °C, substantially below the brittleness threshold of 55 °C. Referring to the base-case results for the end of storage, the PCT was 38.8 °C. This implies that all cladding temperatures may fall below the brittleness threshold at the end of licensing.

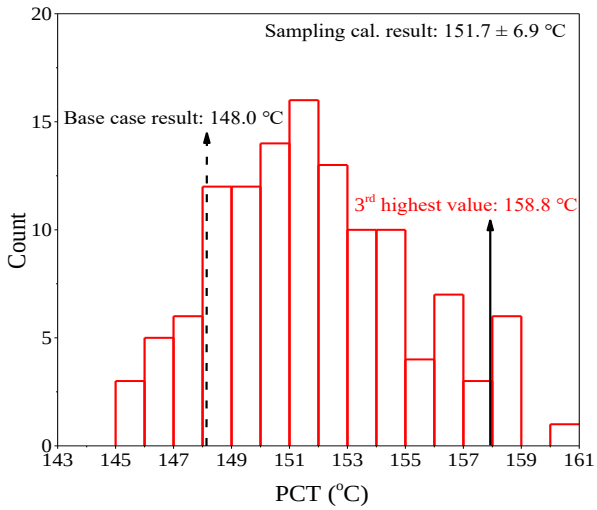

Fig. 5. Distribution of the PCTs from 124 calculations.

Table II: Sensitivity analysis results of the parameters for the PCT.

Rank	Parmeter	Pearson's coefficient
1	C_4 : Radiant heat transfer at the outer wall	-0.72
2	C_3 : Convective heat transfer at the outer wall	-0.39
3	Decay heat per basket at the beginning	0.31
4	Ambient temperature at summer	0.29
5	$\epsilon_{canister}$	-0.27
6	$k_{concrete}$	-0.23
7	Radial ETC	-0.13
8	k_{air}	-0.12
9	$k_{carbon\text{-}steel}$	-0.11
10	C_1 : Convective heat transfer in the canister	-0.11
11	C_2 : Radiant heat transfer in the canister	0.10
12	$k_{stainless\text{-}steel}$	0.09
13	ϵ_{basket}	-0.09
14	μ_{air}	0.09
15	Axial ETC	-0.07
16	ϵ_{liner}	-0.06

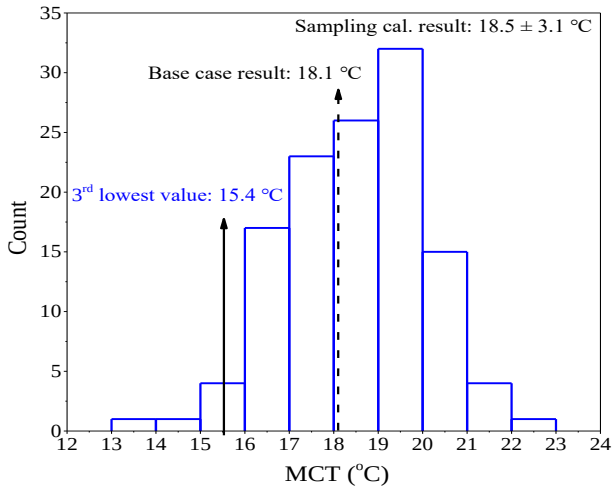

Fig. 6. Distribution of the MCTs from 124 calculations.

Table III: Sensitivity analysis results of the parameters for the MCT.

Rank	Parmeter	Pearson's coefficient
1	Ambient temperature at winter	0.95
2	C_4 : Radiant heat transfer at the outer wall	-0.25
3	C_1 : Convective heat transfer in the canister	-0.18
4	$k_{carbon\text{-}steel}$	0.16
5	$k_{concrete}$	-0.14
6	Axial ETC	0.14
7	Decay heat per basket at the end	0.12
8	μ_{air}	0.12
9	$k_{stainless\text{-}steel}$	0.07
10	$\epsilon_{canister}$	0.06
11	C_2 : Radiant heat transfer in the canister	-0.05
12	ϵ_{liner}	0.05
13	k_{air}	-0.04
14	C_3 : Convective heat transfer at the outer wall	-0.01
15	ϵ_{basket}	0.01
16	Radial ETC	0.01

5. Conclusions

We have predicted the peak and minimum cladding temperatures at CANDU spent fuel canister throughout the licensing duration, utilizing the FLUENT code alongside an uncertainty analysis. The anticipated PCT during this period is estimated at 159.8°C, showing an sufficient safety margin relative to the design criteria. The anticipated MCT during the same timeframe has been assessed at 14.4°C, suggesting that the fuel cladding might turn brittle when the end of licensing period.

REFERENCES

[1] KHNP, Safety analysis report for wolsong unit 1 spent nuclear fuel dry storage facilities, Korea Hydro & Nuclear Power Co., Ltd. CRI, 2004.
[2] KEPCO, Project safety analysis report spent fuel dry storage wolsung nuclear power plant #1, 1990.
[3] M.C. Billone, T.A. Burtseva, Y. Yan, Ductile to brittle transition temperature for high burnup zircaloy-4 and ZIRLO cladding alloys exposed to simulated drying-storage conditions., USNRC, Argonne National Lab., 2013.
[4] KEPCO, Thermal analysis of wolsung unit 1 spent fuel interim storage canister, 1992.
[5] T.G. Lee, T. Kim, T. Na, B. Yun, J.J. Jeong, Realistic thermal analysis of the CANDU spent fuel dry storage canister, Nucl. Eng. Technol. (2023). https://doi.org/10.1016/j.net.2023.08.039.
[6] T.-G. Lee, J.-J. Jeong, Y.-D. Kim, T.-H. Na, Preliminary Assessment of Thermal characteristics of CANDU spent fuel dry storage silo facility using CFD code, J. Energy Eng. 32 (2023) 36–47. https://doi.org/10.5855/ENERGY.2023.32.1.036.
[7] T.J. Baker, FLUENT user's guide, (2021).
[8] KINS, Audit calculatation for the LOCA methodology for KSNP, 2006.
[9] H. Glaeser, GRS method for uncertainty and sensitivity evaluation of code results and applications, Sci. Technol. Nucl. Install. 2008 (2008) 1–7. https://doi.org/10.1155/2008/798901.
[10] J.C. Helton, J.D. Johnson, C.J. Sallaberry, C.B. Storlie, Survey of sampling-based methods for uncertainty and sensitivity analysis, Reliab. Eng. Syst. Saf. 91 (2006) 1175–1209. https://doi.org/10.1016/j.ress.2005.11.017.
[11] F. D'auria, N. Debrecin, G.M. Galassi, Outline of the uncertainty methodology based on accuracy extrapolation, Nucl. Technol. 109 (1995) 21–38. https://doi.org/10.13182/NT109-21.
[12] T.H. Andres, Sampling methods and sensitivity analysis for large parameter sets, J. Stat. Comput. Simul. 57 (1997) 77–110. https://doi.org/10.1080/00949659708811804.
[13] C. Frepoli, An overview of westinghouse realistic large break LOCA evaluation model, Sci. Technol. Nucl. Install. 2008 (2008) 1–15. https://doi.org/10.1155/2008/498737.
[14] F. D'Auria, Best-Estimate Plus Uncertainty (BEPU) approach for accident analysis, in: Therm.-Hydraul. Water Cool. Nucl. React., Elsevier, 2017: pp. 905–950. https://doi.org/10.1016/B978-0-08-100662-7.00014-2.
[15] S.S. Wilks, Determination of sample sizes for setting tolerance limits, Ann. Math. Stat. Vol. 12 (1941) 91–96.
[16] R.R. Rhinehart, R.M. Bethea, Applied engineering statistics, 2nd ed., CRC Press, Boca Raton, 2021. https://doi.org/10.1201/9781003222330.

[17] TRW Environmental Safety Systems, Inc., Spent nuclear fuel effective thermal conductivity report, 1996. https://doi.org/10.2172/778872.
[18] G. Zigh, J. Solis, Computational fluid dynamics best practice guidelines for dry cask applications, Office of Nuclear Regulatory Research, Office of Nuclear Material Safety and Safeguards, 2013.
[19] A.G. Croff, A user's manual for the ORIGEN2 computer code, ORNL, 1980.
[20] K.H. Lee, J.H. Yoon, K.-M. Chae, B.I. Choi, H.Y. Lee, M.J. Song, G. Cho, Evaluation of maximum allowable temperature inside basket of dry storage module for CANDU spent fuel, (n.d.).
[21] Korea Meteorological Administration, 2011-2023 Gyeongju area weather report, Korea Meteorological Administration, 2023. https://data.kma.go.kr/.
[22] 10 CFR 51, 2022.
[23] S.T. Thynell, Discrete-Ordinates method in radiative heat transfer, Int. J. Eng. Sci. 36 (1998) 1651–1675. https://doi.org/10.1016/S0020-7225(98)00052-4.
[24] B.F. Blackwe, W. Gi, K.J. Dowding, R.G. Easterling, Uncertainty estimation in the determination of thermal conductivity of 304 stainless steel, (n.d.).
[25] R. Wyczolkowski, D. Strychalska, V. Bagdasaryan, Correlations for the thermal conductivity of selected steel grades as a function of temperature in the range of 0–800◦C, Arch. Thermodyn. Vol. 43 (2022) 29--45. https://doi.org/10.24425/ather.2022.143170.
[26] M. M. Otha, The concrete canister program, Whiteshell nuclear research establishment, 1978.
[27] K. Kadoya, N. Matsunaga, A. Nagashima, Viscosity and thermal conductivity of dry air in the gaseous phase, J. Phys. Chem. Ref. Data 14 (1985) 947–970. https://doi.org/10.1063/1.555744.